ELSEVIER

Journal of Alloys and Compounds 300–301 (2000) 407–413

Journal of ALLOYS AND COMPOUNDS

www.elsevier.com/locate/jallcom

Crystal field analysis of Er^{3+}-doped glasses: germanate, silicate and ZBLAN

M. Mortier*, Y.D. Huang, F. Auzel

Groupe d'Optique des Terres Rares, CNRS-LPCM, 1 place Aristide Briand, 92195 Meudon, France

Abstract

A simple model of average crystal field Hamiltonian based on the principle of descending symmetry and using the group chain scheme is proposed to describe the average of local symmetries occupied by rare earth ions in a disordered medium. Only three crystal field parameters, one for each rank, have to be fitted in this Hamiltonian. Based on the absorption and emission spectra measured in a conventional way at 13 K, the Stark levels in manifolds from $^4I_{15/2}$ to $^2G(1)_{9/2}$ of Er^{3+} in two oxide glasses: germanate and silicate and one fluoride glass: ZBLAN, are investigated. The scalar crystal field strength is analysed, and former models about optical properties of rare earth ions in glasses are discussed. The crystal field strength is decreasing from silicate to germanate and finally to fluoride glass. In the oxide glasses, the rare earth ions can occupy positions with symmetries distorted from D_4, D_{4h} and their isomorphic groups. In the fluoride glass, the rare earth ions can occupy positions more freely with symmetries distorted from D_4, D_{4h} and also from D_3, D_{3d} and their isomorphic groups. In all studied glasses, the cubic crystal field terms give the major contribution to the crystal field strength around the Er^{3+} ion when the weak axial distortion removes completely the degeneracy.

Keywords: Luminescence; Optical properties; Crystal and ligand fields; Amorphous materials

1. Introduction

Erbium-doped glasses play an important role in the optical communication systems and their crystal field analysis remains still an accurate problem that we will try to treat. This work is based on the following facts: glass material is a disordered medium offering a broad diversity of sites, and then of local symmetries, to receive rare earth ions. The characterization of each type of sites would require a big experimental work with adapted techniques [1,2] due to the intrinsic inhomogeneous broadening of disordered mediums. In a crystal, generally containing a small number of well defined sites for the rare earth ions, rigorous crystal field calculations necessitate a complex and sophisticated modeling [3]. Therefore, the most adapted way for the crystal field study in glasses seems to be a simplified approach more than a sophisticated one. Then, for the experimental side, the inhomogeneous structure of each line will not be tentatively resolved but all the Stark levels corresponding to the manifolds up to 25 000 cm^{-1} will be characterized by classical absorption and emission measurements at low temperature in order to reduce the homogeneous broadening. The modeling will try to analyze the effective symmetry of the ion in the glass, i.e. the average of the real local symmetries, by the position of all these Stark levels. For such an effective Hamiltonian, a high refinement is not useful and the frame of the point charge model has been chosen. Moreover, the application of the descending symmetry principle [4,5], through the group chain scheme [6], allows, with the choice of well adapted basis functions, a simple expression of the crystal field Hamiltonian of the ion in the glass with few parameters.

Two families of oxide glasses and one fluoride glass have been chosen. The coordination of rare earth ions is quite different in fluoride glasses and in oxide glasses as well as the phonon energy range. Consequently, the optical properties of rare earth ions in these three kinds of glasses have noticeable differences. The position and width of Stark levels for Er^{3+} ions in these glasses have been determined from the analysis of their conventional absorption and emission spectra recorded at 13 K.

2. Experimental

The samples, i.e. germanate, silicate and ZBLAN glasses of formulas GeO_2–BaO–K_2O, SiO_2–Na_2O and ZrF_4–BaF_2–LaF_3–AlF_3–NaF, respectively, were cooled to 13 K

*Corresponding author.

E-mail address: mortier@cnrs-bellevue.fr (M. Mortier)

0925-8388/00/$ – see front matter
PII: S0925-8388(99)00753-7

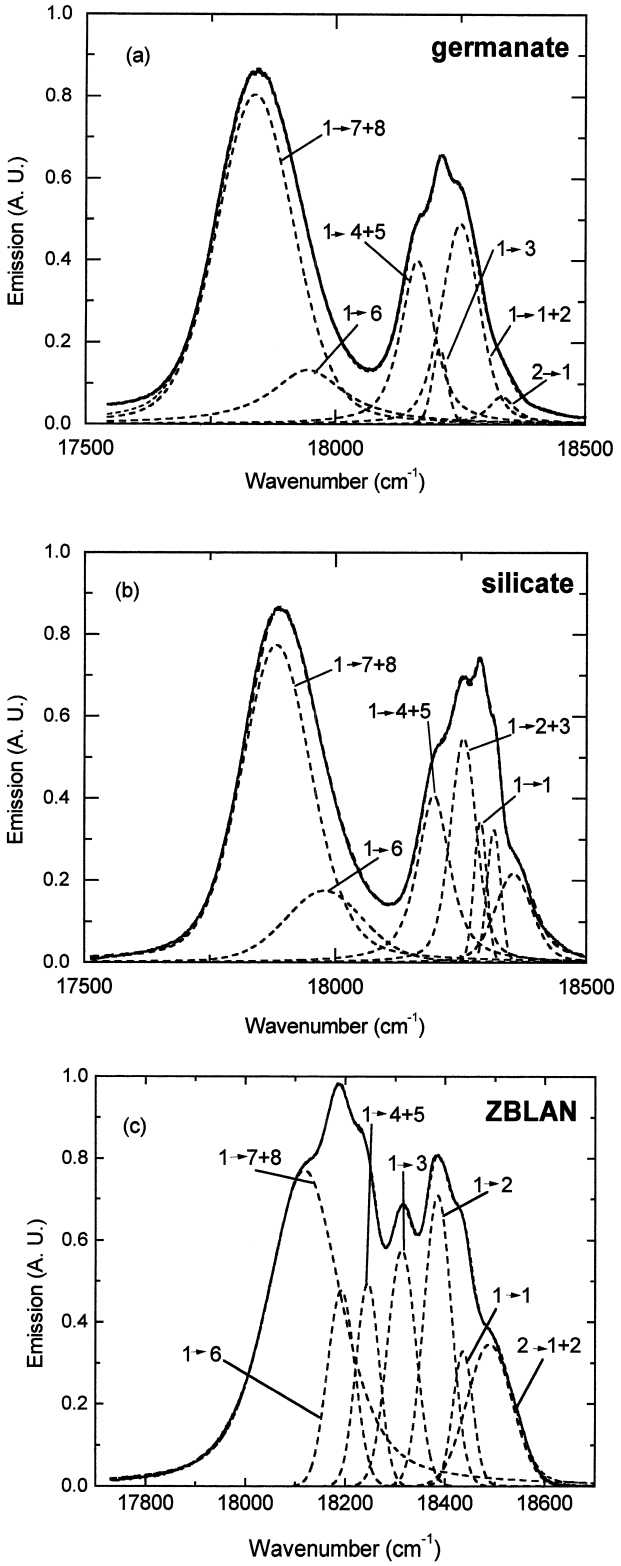

Fig. 1. Voigt profiles fit of the emission spectra associated to the $^4S_{3/2} \rightarrow {}^4I_{15/2}$ transition of Er^{3+} at 13 K. (a) Germanate, (b) silicate, and (c) ZBLAN.

in a He close-cycle cryogenerator. Absorption spectra of Er^{3+} ions have been recorded on a Cary 17 spectrometer in the range from 400 to 1600 nm corresponding to the transitions from $^4I_{15/2} \rightarrow {}^2G(1)_{9/2}$ to $^4I_{15/2} \rightarrow {}^4I_{13/2}$. The 488-nm output from a Coherent Innova 90 Ar^+ ion laser was used to excite Er^{3+} ions in their $^4F_{7/2}$ state. Fluorescence spectra corresponding to $^4S_{3/2} \rightarrow {}^4I_{15/2}$, $^4I_{13/2}$, $^4F_{9/2} \rightarrow {}^4I_{15/2}$, $^4I_{11/2} \rightarrow {}^4I_{15/2}$, and $^4I_{13/2} \rightarrow {}^4I_{15/2}$ transitions were measured in the three glasses. The emission for $^4S_{3/2} \rightarrow {}^4I_{11/2}$ transition was only detected in the germanate glass. A S20 photomultiplier tube, a PIN photodiode and a Northcoast Ge detector were used to cover the whole emission range and placed at the exit slit of a Jobin Yvon HRD monochromator.

The absorption and emission spectra recorded at 13 K were deconvoluted into Voigt-type components. The central position, full width at half the maximum (FWHM) and area of each separated spectral line, and the base line for a whole spectral band were determined. At this temperature, the higher levels in manifolds have very low populations and the spectra are predominated by the transitions from the lowest levels in manifolds. As an example, Fig. 1 shows the Voigt peaks fit to the emission spectra of $^4S_{3/2} \rightarrow {}^4I_{15/2}$ transition for Er^{3+} ions in germanate (Fig. 1a), silicate (Fig. 1b) and ZBLAN (Fig. 1c), respectively. The spectral lines corresponding to transitions from lower Stark level (level 1 in Fig. 1) in $^4S_{3/2}$ to all Stark levels (level 1–8 in Fig. 1) in $^4I_{15/2}$ are pointed out. Previous studies [1,6–12] on Eu^{3+} ions in glasses have shown that, due to the low point symmetries of the sites occupied by RE ions, the manifolds of the ions have full splitting. For Er^{3+} ions, the J manifold splits into $(2J+1)/2$ Stark levels taking into account the Kramers degeneracy. Since some spectral lines are experimentally merged due to the large inhomogeneous width, the FWHM, the area under spectral line corresponding to the intensity of transition and the number of expected lines have been taken into account. For the lines with extreme large values of FWHM and area, more than one transition can be reasonably involved in the line. Some of the mixed lines have been separated after the complete deconvolution of all the experimental spectra. The central positions of the Stark levels for Er^{3+} ions in ZBLAN glasses obtained from the deconvolution are listed in Table 1. The deviations between the deconvoluted and experimental profiles are around 12 cm^{-1}.

3. Energy level analysis

The crystal field theory used in this paper is the point charge model with purely electrostatic interactions between rare earth ion and its ligands. Bond covalency terms are neglected, and neither the spatial extent of the electron clouds nor orbital overlap are formally considered [13,14].

Table 1
Position and width of Stark levels of Er^{3+} ions in ZBLAN at 13 K (cm^{-1})

Manifold	From experimental spectra				Calculated Stark splitting[b]		
	Level position[a]		Stark splitting[a]		$H^{glass}_{cf(D_4)}$	$H^{glass}_{cf(D_3)}$	Average[c]
$^4I_{15/2}$	0		−168.3		−119.1	−150.1	−134.6
	47		−121.6		−109.6	−113.1	−111.4
	111		−57.2		−89.5	−54.1	−71.8
	154		−14.3		−40.9	−49.6	−45.3
	194		25.2		−34.0	−34.6	−34.3
	226		57.3		60.4	116.0	88.2
	308[d]	275	139.5[d]	106.6	158.6	138.6	148.6
	308[d]	341	139.5[d]	172.5	174.1	146.9	160.5
$^4I_{13/2}$	6542		−103.0		−85.1	−120.0	−102.6
	6569		−76.0		−83.7	−64.4	−74.1
	6603		−42.4		−46.5	−35.4	−40.9
	6631		−14.4		−21.7	−29.3	−25.5
	6696	6677[d]	50.6	31.9[d]	17.0	80.7	48.8
	6696	6715[d]	50.6	69.3[d]	110.0	82.2	96.1
	6780		134.6		110.0	86.2	98.1
$^4I_{11/2}$	10 228		−51.1		−52.6	−72.4	−62.5
	10 289	10 267[d]	10.2	−11.8[d]	−38.1	−30.4	−34.3
	10 289	10 285[d]	10.2	6.2[d]	−15.0	−15.8	−15.4
	10 289	10 289[d]	10.2	10.2[d]	−8.9	36.4	13.7
	10 289	10 293[d]	10.2	14.2[d]	54.0	38.2	46.1
	10 289	10 311[d]	10.2	32.2[d]	60.8	44.1	52.4
$^4I_{9/2}$	12 413		−118.4		−80.3	−82.2	−81.3
	12 472		−59.4		−74.1	−72.8	−73.4
	12 538		6.6		16.1	17.8	17.0
	12 617[d]	12 604	85.6[d]	72.5	65.7	67.9	66.8
	12 617[d]	12 630	85.6[d]	98.7	72.6	69.3	70.9
$^4F_{9/2}$	15 271		−85.0		−75.7	−90.9	−83.3
	15 301		−55.0		−51.8	−57.0	−54.4
	15 361		5.0		−4.2	15.4	5.6
	15 398		42.0		20.1	46.5	33.3
	15 449		93.0		111.7	86.0	98.9
$^4S_{3/2}$	18 429		−47.8		−27.9	−27.9	−27.9
	18 525		47.8		27.9	27.9	27.9
$^2H(2)_{11/2}$	19 160		−87.2		−65.2	−63.1	−64.1
	19 203		−44.2		−58.5	−60.3	−59.4
	19 235		−12.2		−10.8	−11.3	−11.0
	19 267		19.8		35.0	34.9	35.0
	19 309[d]	19 300	61.8[d]	52.8	39.3	39.1	39.2
	19 309[d]	19 318	61.8[d]	70.8	60.1	60.7	60.4
$^4F_{7/2}$	20 541		−62.3		−71.8	−58.7	−65.3
	20 586		−17.3		−14.6	−16.7	−15.6
	20 643	20 619[d]	39.8	15.4[d]	28.0	−1.0	13.5
	20 643	20 667[d]	39.8	64.2[d]	58.4	76.4	67.4
$^4F_{5/2}$	22 244		−19.3		−29.8	−17.1	−23.4
	22 273		9.7	0.3[d]	0.5	−17.0	−8.2
	22 273	22 282[d]	9.7	19.1[d]	29.2	34.1	31.6
$^4F_{3/2}$	22 571	22 264[d]	−46.5		−40.8	−40.8	−40.8
	22 664		46.5		40.8	40.8	40.8
$^2G(1)_{9/2}$	24 545		−82.2		−71.1	−74.5	−72.8
	24 582		−45.2		−60.1	−58.9	−59.5
	24 631		3.8		12.5	17.4	14.9
	24 689	24 679[d]	61.8	51.7[d]	49.5	55.7	52.6
	24 689	24 699[d]	61.8	71.9[d]	69.2	60.3	64.7
RMS dev.					21.3	21.6	18.9

[a] For the condition where two levels mix together, another possible choice is given by: $w = (w1 + w2)0.7$ and $w1 = w2$, so $w = 1.4w1$, then $xc1 = xc - 0.3w1$, $xc2 = xc + 0.3w2$, where w is the width and xc the position of the level.

[b] From calculations based on the model $H^{glass}_{cf(D_4)}$ given by Eq. (2) and $H^{glass}_{cf(D_3)}$ given by Eq. (3), and the parameters $C_{k\mu 0}$ were obtained by analyzing the scalar crystal field strength through Eq. (4).

[c] The average values of Stark splittings calculated by $H^{glass}_{cf(D_4)}$ and $H^{glass}_{cf(D_3)}$.

[d] Levels are chosen according to the crystal field analysis.

3.1. Symmetry choice

The average site symmetry C_{2v} is generally used in the crystal field analysis of RE ions in glasses [1,6–12]. This choice was justified by three reasons: (1) it is the highest symmetry allowing the full splitting of the Stark levels, (2) it is a subgroup of almost all the higher point symmetries, and (3) it was, at that time, the lowest symmetry for which simple crystal field calculation could be performed. The bases for choosing C_{2v} to describe the crystal field around rare earth ions are not very sound. This model only allows optical transition for four of the five observed $^5D_0-^7F_2$ components. At the same time, we know that the RE ions in glasses occupy various sites with lots of different environments and then different types of point group. To relate the spectral properties and the coordination of rare earth ions in glasses, the group chain scheme [6] has to be considered.

The irreducible representations of the point symmetry groups can be clearly used as good quantum numbers to label the different Stark levels [15] since no crystal field interactions can occur between states belonging to different irreducible representations when the point symmetry is well defined. Butler [6] has introduced a group–subgroup chain scheme to express the wavefunctions of Stark levels in the irreducible representations. In the group chain scheme, the point symmetry of an active ion can be considered as descending from a highest symmetry, i.e. the full rotation group O_3 or the pure rotation in 3D-space SO_3 ($O_3 = SO_3 \times C_i$) for free ion, to the lower point symmetries (subgroups) step by step and finally to the symmetry at the position occupied by the active ion in crystal. From group theory, we know that the terms of H_{cf} for a point group will exist in the H_{cf} of its subgroup. Therefore, the terms of H_{cf} for high point symmetry, e.g. O, will appear in most of the H_{cf} for different point symmetry groups occupied by rare earth ions. When the eigenfunction of Stark level is expressed in the irreducible representations of the considered point symmetry, contrary to the conventional method [13–15], the crystal field parameters are expressed as the expansion coefficient of H_{cf} according to the irreducible representation wavefunctions [16]. As an example, for the D_4 group, considering the group chain $SO_3 \supset O \supset D_4$,$H_{cf}$ can be expressed as:

$$H_{cf} = \sum_{k,\mu} C_{k\mu 0} b_{k\mu 0} \tag{1}$$

where $k = 2,4,6$ are the rank and are also the irreducible representations of group SO_3, μ are the irreducible representations of O which will be changed or decomposed into the scalar irreducible representation 0 of D_4, $b_{k\mu 0}$ are the basic functions in the space of H_{cf} expressed in the irreducible representations of the group chain $SO_3 \supset O \supset D_4$ and are associated with $|k\mu 0\rangle$ in Ref. [6], and $C_{k\mu 0}$ are the expansion coefficients of H_{cf} according to these bases.

Contrary to the reason of choosing C_{2v}, which is a subgroup of almost all the higher point symmetries, we then consider the high point symmetry group with many subgroups of lower point symmetries in order to describe the average crystal field of rare earth ions in glasses. Moreover, a glass being a highly isotropic medium, no reason appears for an axial symmetry choice. Because a given group G, its isomorphic groups and its rotation–inversion group $G_i = G \times C_i$, have the same mathematical expression of H_{cf} [17], we first choose O (also T_d and O_h, they have the same expression of $H_{cf}{}^{20}$) as the higher point symmetry group (see Fig. 2). In group chain scheme, the H_{cf} of O point symmetry H_{cf}^{O} has only two terms, one for $k = 4$ and the other for $k = 6$, which will express the major terms of corresponding rank of H_{cf} for rare earth ions in glass H_{cf}^{glass}. The term of $k = 2$ appears from symmetries D_4 (also C_{4v}, D_{2d}, and D_{4h}) and D_3 (also C_{3v} and D_{3d}) to lower symmetry, so there are two possible choices for this term. After these considerations, the H_{cf}^{glass} may be written in a 'simplified' group chain [6,16] $SO_3 \supset O \supset D_4$ as:

$$H_{cf(D_4)}^{\text{glass}} = C_{220} b_{220} + C_{400} b_{400} + C_{600} b_{600} \tag{2}$$

or $SO_3 \supset O \supset D_3$ as

$$H_{cf(D_3)}^{\text{glass}} = C_{2\tilde{1}0} b_{2\tilde{1}0} + C_{400} b_{400} + C_{600} b_{600} \tag{3}$$

In these equations, the terms $C_{400}b_{400}$ and $C_{600}b_{600}$ belong to the H_{cf}^{O} and still exist in the H_{cf} of its subgroups D_4 and D_3. Clearly, in the expressions of H_{cf}^{glass}, only three crystal field parameters C_{220} (or $C_{2\tilde{1}0}$), C_{400} and C_{600}, one for each k, will be fitted by the values of Stark splittings.

From Eq. (9.3.7) in Ref. [6], it can be easily shown that the relationship between the crystal field parameters of the conventional JM scheme [15] B_{kq} and the group chain scheme $C_{k\mu 0}$ are:

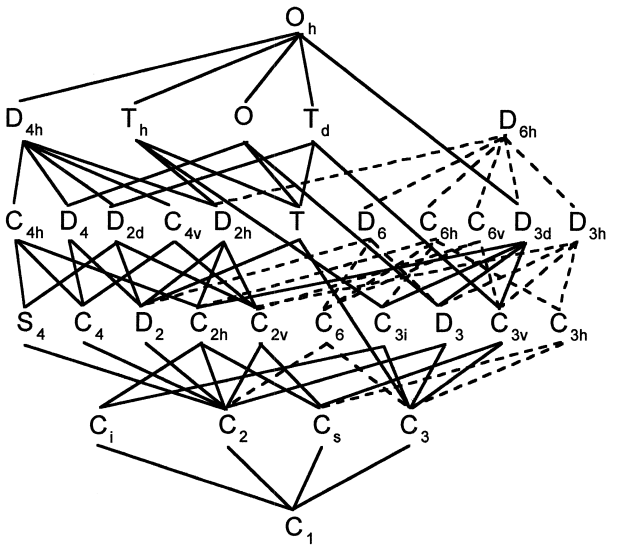

Fig. 2. Imbedding of the crystallographic point groups showing the relations between group and subgroup [6].

For D_4 point symmetry

$$C_{220} = -B_{20}$$

$$C_{400} = \frac{1}{2}\sqrt{\frac{7}{3}}B_{40} + \sqrt{\frac{5}{6}}B_{44}$$

$$C_{420} = \frac{1}{2}\sqrt{\frac{5}{3}}B_{40} - \sqrt{\frac{7}{6}}B_{44}$$

$$C_{600} = -\frac{1}{2\sqrt{2}}B_{60} + \frac{\sqrt{7}}{2}B_{64}$$

$$C_{620} = \frac{1}{2}\sqrt{\frac{7}{2}}B_{60} + \frac{1}{2}B_{64}$$

and for D_3 point symmetry

$$C_{2\tilde{1}0} = -B_{20}$$

$$C_{400} = -\frac{\sqrt{21}}{9}B_{40} - \frac{2\sqrt{30}}{9}B_{43}$$

$$C_{4\tilde{1}0} = -\frac{2\sqrt{15}}{9}B_{40} + \frac{\sqrt{42}}{9}B_{43}$$

$$C_{600} = -\frac{4\sqrt{2}}{9}B_{60} + \frac{2\sqrt{105}}{27}B_{63} - \frac{\sqrt{462}}{27}B_{66}$$

$$C_{6\tilde{1}_0 0} = \frac{\sqrt{462}}{21}B_{63} + 2\sqrt{\frac{5}{21}}B_{66}$$

$$C_{6\tilde{1}_1 0} = \frac{7}{9}B_{60} + \frac{8\sqrt{210}}{189}B_{63} - \frac{8\sqrt{231}}{189}B_{66}$$

Some of these parameters (C_{420},C_{620},$C_{4\tilde{1}0}$,$C_{6\tilde{1}_0 0}$,$C_{6\tilde{1}_1 0}$) are only used in the classical $H_{cf}^{D_4}$, $H_{cf}^{D_3}$ Hamiltonian and not in the H_{cf}^{glass} effective one.

3.2. Scalar crystal field strength

The N_v scalar parameter was introduced to analyze the strength of crystal field for rare earth ions in crystals and glasses whatever the symmetry [18]. From this idea of a scalar crystal field parameter, the relationship between maximum splitting of a manifold, i.e. the separation between the highest and lowest Stark levels in the manifold ΔE, and the average crystal field parameters $C_{k\mu 0}$ for rare earth ions in glasses is:

$$(\Delta E) = \frac{12g_a^2}{g(g_a+2)(g_a+1)} \times \sum_{k=2,4,6} \frac{|\langle [SLJ]\|U^{(k)}\|[SLJ]\rangle|^2 |\langle f\|C^{(k)}\|f\rangle|^2}{2k+1} (C_{k\mu 0})^2 \qquad (4)$$

For Er^{3+} ions, we calculate the $k=2$, 4 and 6 contributions to the overall crystal field strength separately and take splitting values of all manifolds into account. g_a is the degeneracy effectively removed by the field: $g_a = g$ if J is integer and $g_a = g/2$ if J is half-integer. The parameters and operators in these expressions are defined in Ref. [18]. The scalar crystal field strength parameter for rare earth ions in glasses is:

$$N_v = \left[\sum_{k=2,4,6} \frac{4\pi}{2k+1} (C_{k\mu 0})^2 \right]^{1/2} \qquad (5)$$

3.3. Calculations and fitting process

In the calculations, the intermediate coupling wavefunctions given by Weber [19] and the values of reduced matrix elements $\langle \alpha SL\|U^{(k)}\|\alpha SL\rangle$ provided in Ref. [20] were used to get the values of $\langle [SLJ]\|U^{(k)}\|[SLJ]\rangle$ and the J-mixing was not taken into account.

To investigate the Stark splitting of Er^{3+} ions in the glasses, the parameters $C_{k\mu 0}$ were first estimated through fitting the Stark splittings directly by the crystal field Hamiltonian of Eqs. (2) or (3) in the conventional way [16]. Simultaneously, Eq. (4) for the scalar crystal field strength could also be used to derive the absolute values of parameters $C_{k\mu 0}$ ($k=2$, 4, 6) by fitting the experimental values of ΔE of all manifolds obtained from Table 1 through a least-squares fitting procedure. Then, the signs of the values were determined by comparing the Stark splittings calculated by Eqs. (2) or (3) and the experimental data. To completely verify our assumption on the Hamiltonian for glass systems H_{cf}^{glass}, a series of H_{cf} for point symmetry O (also T_d and O_h), H_{cf}^{O}; D_4 (also C_{4v}, D_{2d} and D_{4h}), $H_{cf}^{D_4}$; D_3 (also C_{3v} and D_{3d}), $H_{cf}^{D_3}$; and D_2 (also C_{2v} and D_{2h}), $H_{cf}^{D_2}$ was also considered in fitting the Stark splittings. For these H_{cf} Hamiltonians, the complete expression including more parameters is used The root-mean-squared (RMS) deviations of all the calculations are shown in Fig. 3a, b and c, respectively, for Er^{3+} ions in germanate, silicate and ZBLAN. Due to the experimental merging of some Stark levels, different possible choices of level structure could be considered. The corresponding range of RMS are represented by the error bars. On the x-axis are distributed the various point symmetries used in the analysis: the positive direction represents the distortion about $O \supset D_4 \supset D_2$, the negative direction represents the distortion about $O \supset D_3$. The classical H_{cf} Hamiltonian are represented by O, D_3, D_4, D_2 and the effective Hamiltonian for glasses by $G(D_3)$ and $G(D_4)$. The distance between different symmetries is determined by the number of the crystal field parameters included in the fitting process, e.g. there are two crystal field parameters for O point symmetry and five for D_4, so the distance between them is three units.

4. Results and discussion

In all cases, the RMS deviations between the experimental data of Stark splitting and the data calculated by H_{cf}^{glass} are almost the same (Fig. 3) for the two ways of calculation, through fitting the maximum splittings of

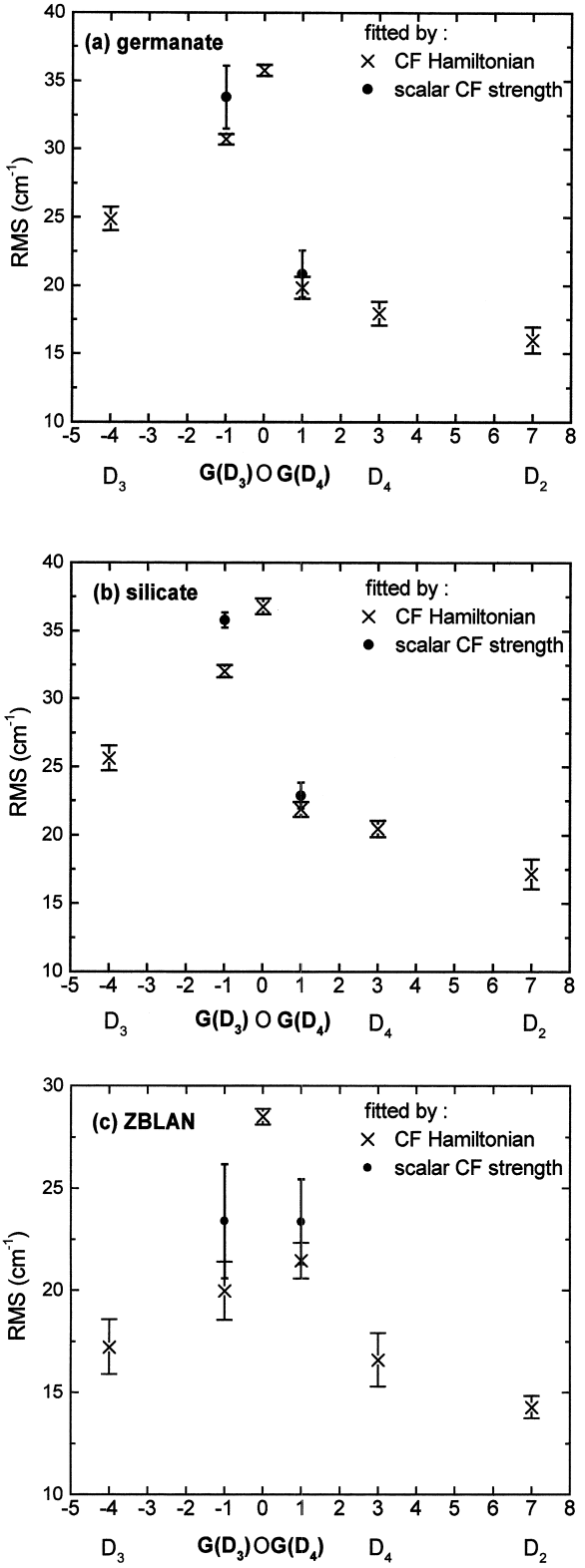

Fig. 3. RMS deviations between experimental and calculated splittings. Calculation by crystal field Hamiltonian of O, D_4, D_3, D_2 point symmetries and the model proposed for glass, $G(D_3)$ and $G(D_4)$. (a) Germanate, (b) silicate, and (c) ZBLAN.

manifolds by Eq. (4) or fitting all of the Stark splittings in conventional way by Eqs. (2) or (3), and the $C_{k\mu 0}$ got by these two different procedures are listed in Table 2 and have very similar values.

For both germanate and silicate glasses, $H^{\text{glass}}_{cf(D_4)}$, $H^{D_4}_{cf}$ and $H^{D_2}_{cf}$ have similar values of RMS although the numbers of adjustable parameters in the Hamiltonian are 3, 5 and 9. $H^{\text{glass}}_{cf(D_4)}$ is much better than $H^{\text{glass}}_{cf(D3)}$ for expressing the average crystal field Hamiltonian of Er^{3+} ions (smaller RMS values in direction $O \supset D_4 \supset D_2$ than in $O \supset D_3$, especially when the number of fitting parameters is considered). Then, Er^{3+} ions occupy preferentially the positions with symmetries distorted from D_4, D_{2d}, C_{4v} and D_{4h} and their isomorphic groups.

In fluoride (ZBLAN) glass, the RMS deviations have similar values in both directions of the group chains $O \supset D_4 \supset D_2$ and $O \supset D_3$. Especially, the deviations for $H^{\text{glass}}_{cf(D_4)}$ and $H^{\text{glass}}_{cf(D_3)}$ are almost the same but decreasing to 18.9 cm^{-1} for the average result (Table 1). The RMS deviations do not decrease remarkably from H^{O}_{cf} to $H^{\text{glass}}_{cf(D_4)}$. In this case, the Er^{3+} ions can equally occupy positions with any kind of point symmetries, i.e. symmetries distorted not only from D_4, D_{4h} and their isomorphic groups but also from D_3, D_{3d} and their isomorphic groups. Then, the effective Hamiltonian for fluoride glass can be expressed in 'higher' point symmetry (such as O) than for oxide glass.

In ZBLAN, the scalar crystal field strength parameter N_v calculated from Eq. (4) lies in the range of 1855–2081 cm^{-1}, so the crystal field is weaker than in oxide glasses where values 2948–2949 cm^{-1} and 3123–3182 cm^{-1} have been obtained for germanate and silicate respectively (see Table 2). The Er^{3+} ions in these two oxide glasses have similar values of $C_{k\mu 0}$ and identical structures of energy levels and then similar average crystal field environments. The crystal field is stronger in silicate glass than in germanate glass although the ligands of Er^{3+} ions are oxygens with a same coordination number in both of the glasses.

It can be interestingly noticed in all cases that the cubic crystal field terms (C_{400}, C_{600}) give the major contribution to the crystal field strength. However, the weak axial contribution (C_{220}) allows the complete degeneracy removing. Such consideration explains why optical transitions between Stark levels of rare earth ions are allowed in glasses as in crystal with low point symmetry but at the same time that the structure of levels displays the feature of 'high' point symmetry.

5. Conclusion

In the conventional way, most of workers had tried to find a pure and low point symmetry to describe the average environment of rare earth ions in glasses. In this paper,

Table 2
Parameters $C_{k\mu 0}$ and N_v derived from observed Stark splittings of Er^{3+} (cm^{-1})

	Germanate		Silicate	
	By ΔE[a]	By Stark levels[b]	By ΔE[a]	By Stark levels[b]
C_{220}	706.2	669.1	683.3	672.2
C_{400}	2274.5	2290.5	2477.7	2535.6
C_{600}	−471.5	−506.6	−95.2	−96.1
N_v	2948	2949	3123	3182
	ZBLAN			
	By ΔE[a]	By Stark levels[b]	By Stark levels[c]	
C_{220}[b] or $C_{2\bar{1}0}$[c]	503.8	509.6	583.5	
C_{400}	1597.6	1376.6	1295.8	
C_{600}	−367.0	−482.9	−497.9	
N_v	2081	1877	1855	

[a] Parameter values obtained through analyzing the scalar crystal field strength by Eq. (4).
[b] Parameter values obtained by $H^{glass}_{cf(D_4)}$ through Eq. (2).
[c] Parameter values obtained by $H^{glass}_{cf(D_3)}$ through Eq. (3).

based on the idea that the disordered structure of glass leads to site-to-site variations of the rare earth sites, an average crystal field Hamiltonian has been introduced by means of the group chain scheme. Although this is a simple model with only three major parameters $C_{k\mu 0}$ for the Hamiltonian, it has permit to explain in a rather realistic way the optical properties of Er^{3+} ions.

Our fitting results have shown that the Hamiltonian $H^{glass}_{cf(D_4)}$ (Eq. (2)) is more suitable than $H^{glass}_{cf(D_3)}$ (Eq. (3)) to describe the average crystal field of Er^{3+} ions in the two oxide glasses investigated.

In the fluoride glass, the rare earth ions can occupy positions more freely than in the oxide glasses. The rare earth ions experiences symmetries distorted not only from D_4, D_{4h} and their isomorphic groups but also from D_3, D_{3d} and their isomorphic groups. As an average result, the Hamiltonian for fluoride glass may have 'higher' point symmetry (such as O) than for oxide glass. Due to the role of rare earth fluorides (RF_3) as intermediate element in these glasses, they are able to be both in and out of network positions. This implies that rare earth ions in fluoride glasses may be more evenly distributed. In return, the rare earth ions can only play a glass-modifier role in oxide glasses.

In all cases, the cubic crystal field terms give the major contribution to the crystal field strength when the weak axial contribution allows the complete degeneracy removing.

Acknowledgements

The authors would like to acknowledge Fabienne Pellé and Philippe Goldner for fruitful discussions.

References

[1] C. Brecher, L.A. Riseberg, Phys. Rev. B 13 (1976) 81.
[2] T.F. Belliveau, D.J. Simkin, J. Non-Cryst. Solids 110 (1989) 127.
[3] D. Garcia, M. Faucher, Crystal field in non-metallic (rare earth) compounds, in: K.A. Gschneider, L. Eyring (Eds.), Handbook on the Physics and Chemistry of Rare Earths, Vol. 21, 1995, p. 263.
[4] F. Auzel, Thèse, Faculté des Sciences de Paris, 1968.
[5] B. Judd, unpublished data.
[6] P.H. Butler, Point Group Symmetry Application: Method and Tables, Plenum Press, New York, 1981.
[7] M. Tanaka, T. Kushida, Phys. Rev. B 49 (1994) 5192.
[8] M.J. Lochhead, K.L. Bray, Phys. Rev. B 52 (1995) 15763.
[9] G. Pucker, K. Gatterer, H.P. Fritzer, M. Bettinelli, M. Ferrari, Phys. Rev. B 53 (1996) 6225.
[10] J. Fernandez, R. Balda, J.L. Adam, J. Phys. Condens. Matter 10 (1998) 4985.
[11] M. Bettinelli, A. Speghini, M. Ferrari, M. Montagna, J. Non-Cryst. Solids 201 (1996) 211.
[12] S. Todoroki, K. Hirao, N. Soga, J. Appl. Phys. 72 (1992) 5853.
[13] J.B. Gruber, J.R. Quagliano, M.F. Reid, F.S. Richardson, M.E. Hills, M.D. Seltzer, S.B. Stevens, C.A. Morrison, Phys. Rev. B 48 (1993) 15561.
[14] K.W. Kramer, H.U. Gudel, R.N. Schwartz, Phys. Rev. B 56 (1997) 13830.
[15] B.G. Wybourne, Spectroscopic Properties of Rare Earths, Wiley, London, 1965.
[16] Z. Luo, Y. Huang, J. Phys. Condens. Matter 6 (1994) 3737.
[17] C.A. Morrisson, R.P. Leavitt, in: K.A. Gschneider (Ed.), Handbook on the Physics and Chemistry of Rare Earths, Vol. 5, North-Holland, Amsterdam, 1982.
[18] F. Auzel, O.L. Malta, J. Phys. 44 (1983) 201.
[19] M.J. Weber, Phys. Rev. 157 (1967) 262.
[20] C.W. Nielson, G.F. Koster, Spectroscopic Coefficients for p^n, d^n and f^n Configurations, MIT, Massachusetts, 1974.